ATMOSPHERIC AEROSOL DETECTION AND ITS REMOVEAL FOR SATELLITE DATA

Dong Ha Lee[1], Kwon Ho Lee[1),2)], Young Joon Kim[1)]

[1)] Advanced Environmental Monitoring Research Center (ADEMRC),
Gwangju Institute of Science & Technology (GIST), dongha@gist.ac.kr, yjkim@gist.ac.kr
[2)] Earth System Science Interdisciplinary Center (ESSIC), University of Maryland (UMD), kwonlee@umd.edu,

ABSTRACT: Satellite imagery may contain large regions covered with atmospheric aerosol. A high-resolution satellite imagery affected by non-homogenous aerosol cover should be processed for land cover study and perform the radiometric calibration that will allow its future application for Korea Multi-Purpose Satellite (KOMPSAT) data. In this study, aerosol signal was separated from high resolution satellite data based on the reflectance separation method. Since aerosol removal has a good sensitivity over bright surface such as man-made targets, aerosol optical thickness (AOT) retrieval algorithm could be used. AOT retrieval using Look-up table (LUT) approach for utilizing the transformed image to radiometrically compensate visible band imagery is processed and tested in the correction of satellite scenery. Moderate Resolution Imaging Spectroradiometer (MODIS), EO-1/HYPERION data have been used for aerosol correction and AOT retrieval with different spatial resolution. Results show that an application of the aerosol detection for HYPERION data yields successive aerosol separation from imagery and AOT maps are consistent with MODIS AOT map.

KEY WORDS: Aerosol, HOT, MODIS, HYPERION

1. INTRODUCTION

Atmospheric aerosol retrieval can provide relative aerosol mass loading in atmosphere as well as information about atmospheric correction for surface monitoring. For last few decades, many instruments including AVHRR, POLDER, SeaWiFS, MISR, and MODIS have been used to study global or regional scale aerosol (King et al., 1999). For local scale study using more high resolution data including typical commercial satellite data, however, aerosol retrieval or aerosol correction is needed over the region of interest (ROI) for more practical applications. As one of those high resolution satellites, Korea Multi-Purpose Satellite (KOMPSAT) was the first joint spacecraft developed by Korea Aerospace Research Institute (KARI). KOMPSAT-2 having 4m resolution Multi Spectral Camera (MSC) was launched on 28 July 2006.

Since the surface reflectance typically increases as the pixel size increases, the error for aerosol retrieval increases. Typical aerosol correction for high resolution satellite data has been used by *in-situ* atmospheric measurements and radiative transfer model (RTM) simulations. However, problems are that *in-situ* measurements are not always provided during satellite passing time and RTM with ground truth data can not applied for wide region because of inhomogeneous aerosol distribution in the atmosphere. Therefore aerosol detection is also important subject for KOMPSAT mission. In this study, we present the results of local scale aerosol detection using HYPERION 30m and MODIS 1km and half km resolution data. Although HYPERION operates in wide hyper-spectral regions (0.23~2.55 μm), the solar reflective bands (Visible and SWIR bands) have been used for aerosol detection in this study. In order to retrieve aerosol optical depth (AOD) over the local scale area, surface reflectance and Look-up table (LUT) constructed from the Santa Babara DISORT Radiative Transfer (SBDART; Ricchiazzi et al. 1998) RTM was used with various aerosol models.

2. METHODOLOGY

This study used HYPERION and MODIS data to detect aerosol and estimate the AOD over Korea (Table 1). Figure 1 shows schematic diagram of the aerosol retrieval algorithm used in this study. In order to process L1b band reflectance HYPERION reflectance data has been calculated from radiance data with extra terrestrial solar irradiance and solar geometry.

Table 1. Datasets used in this study

Setting	HYPERION	MODIS
Date	3 April 2002	3 April 2002
Time	02:00~02:01	02:25~02:30
Bands	11, 21, 31, 51, 198	1,2,3,4,7
Wavelengths	467,559,660, 864,2133nm	660,865,465, 555, 2130nm
Resolution	30m	1km, Hkm

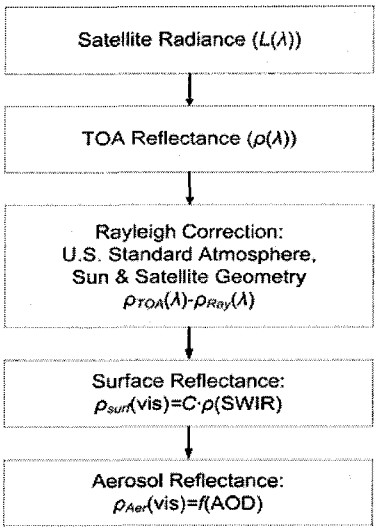

Figure 1. Flow chart of aerosol detection algorithm.

$$\rho_{TOA}(\lambda) = \frac{\pi \cdot L_{TOA}(\lambda)}{F_0(\lambda) \cdot \cos(\theta_{sun})} \quad (1)$$

Where ρ_{TOA} = reflectance at TOA
L_{TOA} = satellite measured radiance
F_0 = Extraterrestrial solar irradiance
θ_{sun} = solar zenith angle

The aerosol detection can be processed in two distinct parts. They are accurate surface reflectance removal from satellite data and aerosol model selection for RTM. At first, TOA reflectance in a cloud-free pixel should be separated from Rayleigh scattering and surface reflectance. Then LUTs were constructed by RTM calculation with various aerosol models. AOT can be retrieved from the inverse process by comparing measured aerosol reflectance to calculated values. The atmospheric effects produced by atmospheric molecules and aerosols are the main contributors in the visible region, as it propagates through the atmosphere. Assuming the ground surface is Lambertian, the radiative transfer equation is,

$$\rho_{TOA} = \rho_{Aer} + \rho_{Ray} + \frac{T_{Sun} \cdot T_{Sat} \cdot \rho_{Surf}}{1 - s \cdot \rho_{Surf}} \quad (2)$$

Where $\rho_{TOA}, \rho_{Aer}, \rho_{Ray}, \rho_{Surf}$ = reflectance at TOA, by aerosol, rayleigh scattering, and surface, respectively.
T_{Sun}, T_{Sat} = the downward and upward total transmittances.
s = the hemispheric spherical albedo.

3. RESULTS AND DISCUSSION

3.1 Rayleigh correction

For the rayleigh correction, For the separation of the Rayleigh scattering from TOA reflectance the Rayleigh optical thickness ($\tau_{Ray}(\lambda)$) can then be determined using U.S. standard atmosphere in each pixel through the following equation (Bucholtz, 1995):

$$\tau_{Ray}(\lambda) = A \cdot \lambda^{-\left(B + C \cdot \lambda + \frac{D}{\lambda}\right)} \quad (3)$$

where A, B, C, D = the constants for the total Rayleigh scattering cross-section and total Rayleigh volume scattering coefficient for a standard atmosphere.

Figure 2 shows a sample of Rayleigh correction results. Over typical water pixels our Rayleigh reflectance calculated with eq (3) and RTM calculated Rayleigh reflectance quite well agreed each other. Difference between TOA and Rayleigh reflectance is aerosol+surface reflectaces. If surface reflectance is near zero then aerosol reflectance could be derived easily.

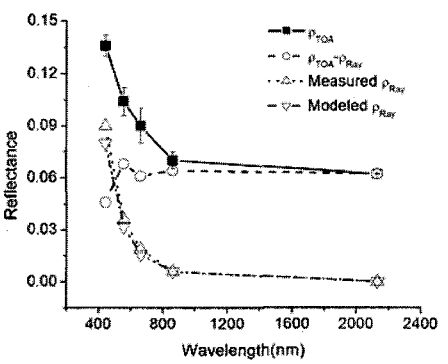

Figure 2. Observed and modelled reflectance from HYPERION over water pixel.

3.2 Surface Reflectance

The surface reflectance is major problem to retrieve aerosol over land. Since it is correlated to some extent in reflected solar radiation, shorter wavelength reflectance could be deduced from that of longer wavelength. Since the aerosol signature is negligible in longer wavelength, the TOA reflectance in the SWIR wavelength can be taken as the ground reflectance. Kaufman et al. (1997) and Kaufman and Sendra (1998) found that there existed empirical band ratios for a land category between the visible reflectance and 2.1 micron reflectance as follows:

$$\rho_{0.66} = 0.5\rho_{2.1}, \ \rho_{0.46} = 0.25\rho_{2.1} \quad (4)$$

Where, ρ_{λ} = reflectance at λ μm

This ratio is currently used for MODIS operational aerosol retrieval over land from NASA. This band correlation method is a useful method for retrieving the aerosol parameters over lands. However, this ratio could be affected by surface cover type and angular orientations.

Furthermore, large particle could be affected on 2.1 micron reflectance. Therefore regional variation in the band reflectance ratio should be checked over study area. Figure 1 shows the regression between visible and SWIR band reflectances for a HYPERION image except for water pixel ($\rho_{0.86}$ <0.1). The regressions are formed by correlating 10x10 pixels. The good linear regressions of the red channels against the SWIR (R=0.87). Since Rayleigh corrected reflectances were used in correlation analysis, remaining aerosol effects may increase intercept of regression line.

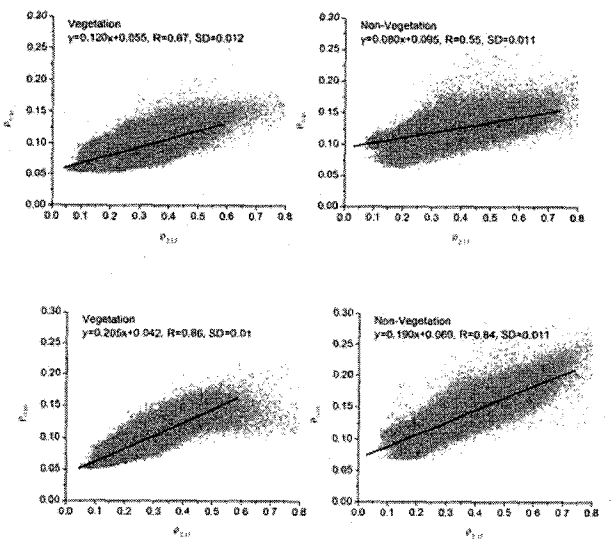

Figure 3. Visible/SWIR ratio for vegetation (NDVI>0.25) and non-vegetation pixels (NDVI<0.25) at 0.46 and 0.66 μm , respectively. Note that reflectance at each wavelength has been corrected Rayleigh scattering and total transmission.

3.3 Aerosol retrieval and comparison

Figure 4 shows the HYPERION retrieved AOD imagery on April 9, 2002. The aerosol reflectances were calculated by subtracting Rayleigh scattering in 3.1 and surface contribution in 3.2 from TOA reflectance in Eq(1). LUT for inverse processing has been calculated by SBDART model. AOD at 446 and 645 nm has been retrieved from satellite observation data. The HYPERION reflectance data at 465nm and 645nm were used to retrieve AOD. AOD at 550nm could be calculated by using angstrom exponent between 446 and 645 nm.

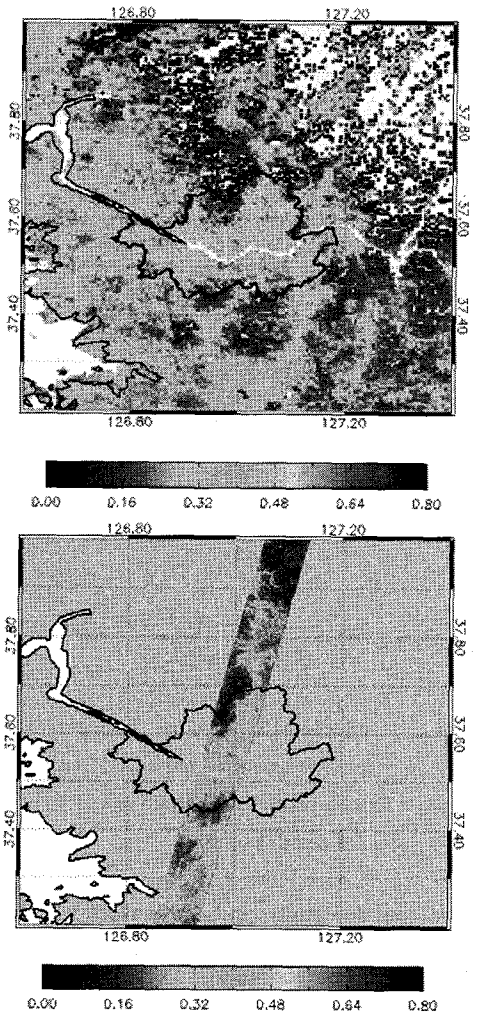

Figure 4. MODIS retrieved AOT (500m resolution) and HYPERION AOT (30m resolution), respectively.

Unfortunately no ground truth data was available, only MODIS retrieved 500m resolution AOD data (Lee et al., 2005) and HYPERION in this study were compared. In Figure 4, relatively good agreement between the MODIS AOD product and aerosol detection result demonstrated in this study.

4. SUMMARY

Reflectance separation method for aerosol retrieval for HYPERION data was used to examine the high resolution satellite image-based aerosol detection. The results show that Rayleigh correction for removal of scattering by atmospheric molecules was accurate. Surface reflectance determination, however, is needed more accuracy for acquisition of aerosol only signal. Although Vis/SWIR correlation method is useful, its variation in terms of various surface conditions should be known for aerosol retrieval. Finally, retrieved aerosol reflectance and AOD

produces promising results comparable to MODIS AOD data. The present results clearly indicate the possibility of aerosol detection and its correction for high resolution satellite image such as KOMPSAT MSC image. Note, however, that the comparisons made during this investigation occurred on days with relatively homogeneous atmospheric conditions. Future work would benefit from having ground measurements and surface. In addition, finding how to obtain the AOD distribution of an entire scene and applying them to compare for air-quality monitoring.

References

Ricchiazzi P, Yang S, Gautier C, Sowle D, 1998, SBDART: A Research and Teaching Software Tool for Plane-Parallel Radiative Transfer in the Earth's Atmosphere. *Bulletin of the American Meteorological Society,* 79(10), pp. 2101–2114.

King, M. D., Kauffman, Y. J., Tanre, D., & Nakajima, T., 1999, Remote sensing of tropospheric aerosols from space: past, present, and future. *Bulletin of the American Meteorological Society*, 80 (11), pp. 2229– 2259.

Lee, K.H., D. H. Lee, Y. J. Kim, J. Kim, 2006, MODIS 500×500m^2 resolution aerosol optical thickness retrieval and its application for air quality monitoring, *Proceeding of 6th International symposium on advanced environmental monitoring*

Bucholtz, A., 1995, Rayleigh-scattering calculations for the terrestrial atmosphere, *Applied Optics,* 34, pp. 2765–2773.

Kaufman, Y.J., Wald, A.E., Remer, L.A., Gao, B.C., Li, R.R., and Flynn, L., 1997, The MODIS 2.1-㎛ channel correlation with visible reflectance for use in remote sensing of aerosol. *IEEE Transactions on Geoscience and Remote Sensing*, 35, pp. 1286-1298.

Kaufman, Y. J., & Sendra, C., 1988, Algorithm for automatic atmospheric corrections to visible and near-IR satellite imagery. *International Journal of Remote Sensing*, 9, 1357– 1381.

Acknowledgements

This work was supported by the Korea Aerospace Research Institute (KARI).